# CATHODOLUMINESCENCE AND MATERIAL CHARACTERIZATION

**M. Nazarov**

*Institute of Applied Physics, Academy of Sciences of Moldova, Academiei str. 5, Chisinau, MD-2028, Republic of Moldova*
*E-mail: mvnazarov@mail.ru*

(Received April 20, 2016)

## Abstract

Some new and nonconventional methods of materials investigation, such as color cathodoluminescence and composite cathodoluminescent and back-scattering electron contrast in SEM, are presented and explained. Advantages of these methods are demonstrated in studying the $SrAl_2O_4:Eu^{2+}$, $Dy^{3+}$ luminescent phosphor and artificial diamonds.

## 1. Introduction

The emission of ultraviolet, visible, or infrared light stimulated by electron bombardment is known as cathodoluminescence (CL; from cathode rays as J. J. Thompson described electrons in 1897). CL was first studied by William Crookes in 1879. He discovered that $CaWO_4$ scheelite placed opposite the cathode in a vacuum discharge tube yielded spectacular fluorescence. He concluded that some particles traveled from the cathode to the target causing the fluorescence well before Thomson discovered the electron. Crookes also studied luminescence from many other minerals (diamond, ruby, sapphire, zircon, etc.). However, systematic observations and discussion of CL did not take place until 1965, when Smith and Stenstrom studied CL with a microprobe [1]. The pioneering CL studies were carried out with a CL microscope, which fundamentally is a petrographic microscope to which a cathode gun is attached. Subsequently, an electron-probe microanalyzer and, especially, a scanning electron microscope were utilized to generate high-resolution high-magnification CL images.

It should be noted that CL-modes being incorporated into a SEM instrument (CL-SEM) give both the spectral and spatial information with high resolution. In geology, mineralogy, and materials science, a scanning electron microscope with specialized optical detectors, or an optical CL microscope, is used to examine internal structures of luminescent materials in order to get information on the composition, growth, and quality of the material. CL in semiconductors occurs because the impingement of a high energy electron beam onto a semiconductor will result in the promotion of electrons from the valence band into the conduction band, leaving behind a hole. Recombination of an electron and a hole provide the emission of a photon. The energy (color) of the photon, as well as the probability of emission of a photon rather than a phonon, depends on the type, purity, and defect state of the material. In this case, the semiconductor examined can, in fact, be almost any non-metallic material. In terms of the band structure, classical semiconductors, insulators, ceramics, gemstones, minerals, glasses, and powders can be treated in the same way.

The luminescence of most phosphors comes from a few sites (activator centers) occupied

by selected chemical impurities incorporated into the matrix or host solid. Direct excitation of the activator is only possible with ultraviolet and/or visible radiation. High-energy electron beam excitation always excites the host lattice. Because of the complex mode of interaction of cathode rays with phosphors, the energy efficiency of light production by CL is lower than the best efficiencies provided by photoluminescence (PL). The main advantage of CL spectroscopy in comparison with PL is the possibility of local measurements with geometrical resolution less than 1 μm, while PL is an integrated mode.

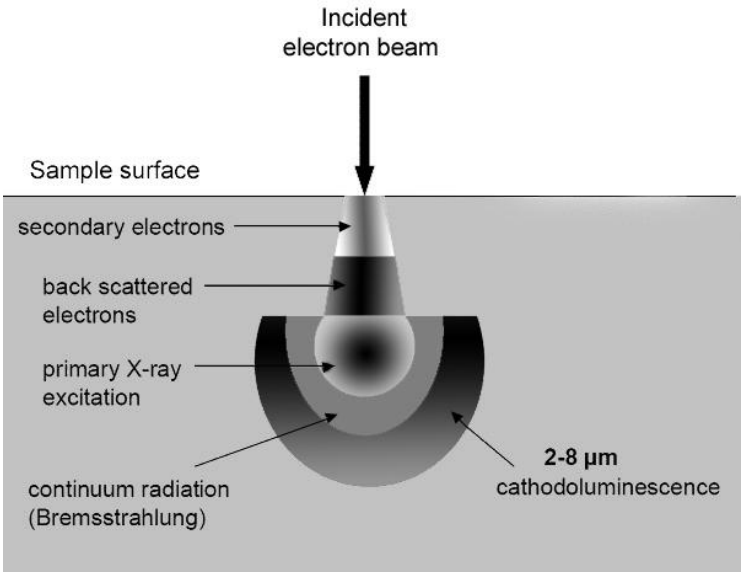


**Fig. 1**. Schematic shapes of electron interaction volumes.

The penetration depth of the incident beam and, therefore, the excited volume in the sample depend on the energy of the incident electrons and the atomic number of the studied material. If secondary and back-scattered electrons are formed from the subsurface layer, CL is typically generated from depths down to 2–8 μm; it is a volume effect. Thus, the geometrical resolution in CL depends not only on electron beam diameter, but also on the CL interaction volume. In fact, it can be about 1 μm. A 3D image of the sample can be obtained if the scanning mode and electron energy variation are combined. Usually, a CL mode is applied in phosphor investigations in combination with other modes in SEM, such as SE or BSE (see the next paragraph).

## 2. Investigation methods

### *2.1 Monochromatic CL*

An example of CL application to a ZnO–Zn powder sample is shown in Fig. 2. The dominant CL emission peak for ZnO–Zn is located at 495 nm.

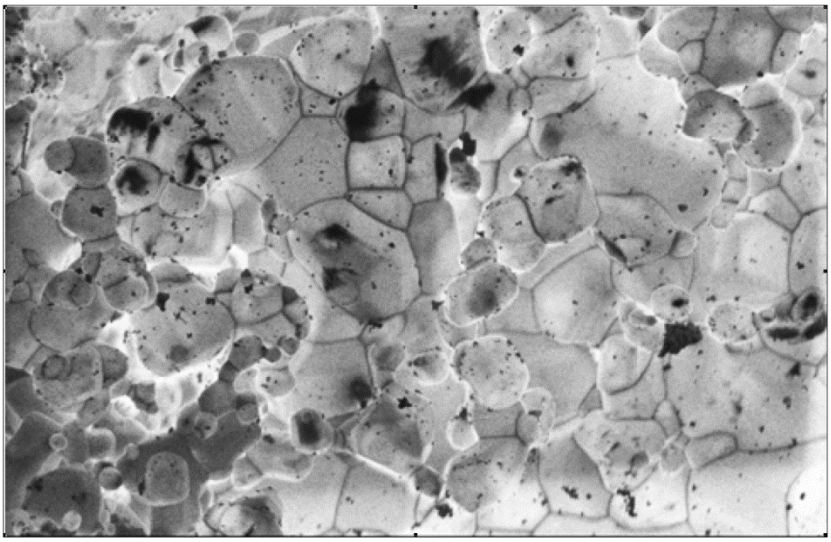

**Fig. 2**. CL image of ZnO–Zn at 495 nm and 1 kV. Horizontal Width of Field (HWF) of 58 μm.

This work has demonstrated the capabilities of low-voltage scanning CL microscopy for high-resolution spatially resolved characterization of the luminescence properties of CL phosphors.

### *2.2 Panchromatic or color CL*

Among the different CL-SEM modes, the most informative is color CL (CCL). The use of color contrast was shown to increase the information content of color images in comparison with the black-and-white counterpart by about two orders of magnitude [2]. Previously, the CCL-SEM mode was used for a complex characterization of different organic, dielectric, and semiconductor luminescent materials [2–5]. Here, we show one of the examples of CCL application to phosphors in a powder form.

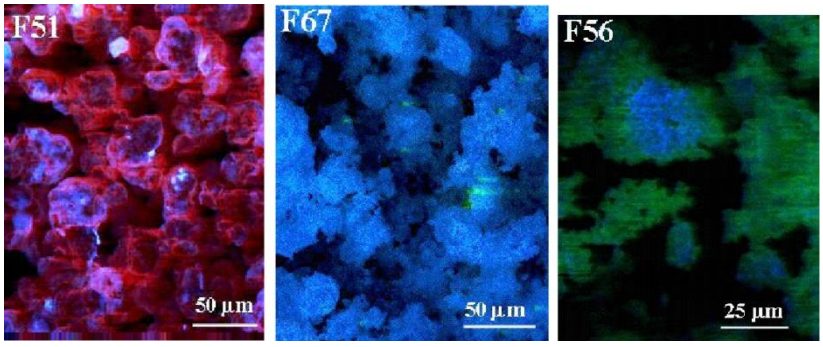


**Fig. 3.** Panchromatic images of nonactivated $CaWO_4$ (F67) and the sample activated with $Eu^{3+}$ (F51) and $Tb^{3+}$ (F56) (original blue color for host lattice emission, red color for Eu incorporations and green for Tb).

Mechanisms leading to the emission of light from phosphors are rather similar for all forms of excitation. In all cases, luminescence arises owing to stimulation of the substance to an

excited state. This excitation involves an input of energy from a source of suitable radiation, e.g., from an electron beam at CL. Solids centers of luminescence contain atoms, ions, or groups of ions located near the lattice imperfections. An imperfection in the host lattice may be produced by introducing an activator or by producing a vacancy. The radiative transition of an excited center to the ground state is accompanied by the emission of light.

A special attachment for CCL-SEM examinations of topography and morphology of powder samples and a CL spectrometer for local CL measurements are shown in Fig. 4.

### *2.3 Composite CL and back-scattering electron contrast in SEM*

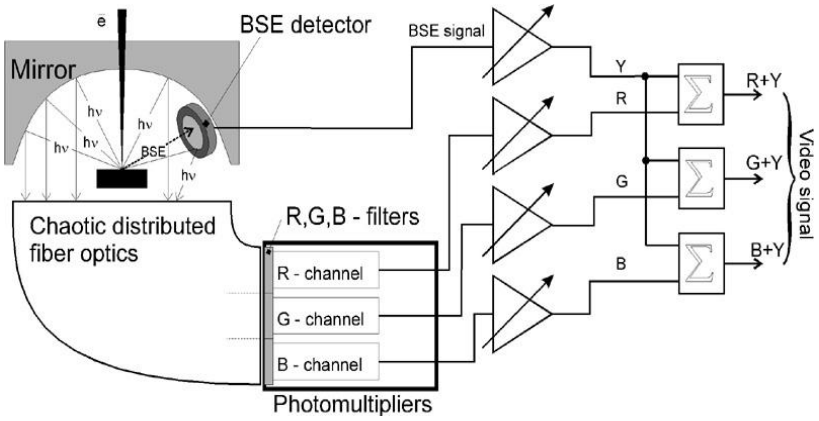


**Fig. 4.** CCL- SEM attachment for CCL.

A schematic diagram of the (CCL+BSE) detector unit in SEM is presented in Fig. 4. The basic equipment comprises a Stereoscan MK-IIA SEM instrument integrated with a CCL light collector and a solid state barrier counter for the measurement of BSE current. The BSE detector is located near the specimens under a parabolic mirror. Undistorted CCL and BSE signals are detected simultaneously during electron beam scanning.

CL is transmitted by optical fibers from the specimen chamber. Later, using three R-, G-, and B-filters, the CL signal is transformed into electric video signals by photomultipliers. These signals are multiplied by preamplifiers which set the amplification ratio and zero value (black level). The BSE detector is integrated with the amplifier and operates at negative bias that increases the electrical and noise stability. The electric potential of the detector body is chosen to be identical with that of the microscope column potential to eliminate its action on the electron beam. The amplifier of the BSE signal also allows varying the amplification factor and the black level of the video signal. After pre-amplification, the R-, G-, B- and BSE (Y)-signals are summed, as shown in Fig. 4. As a result, we have three video signals: R+Y, G+Y, and B+Y, which are transformed into digital form and are displayed on the computer screen. The above-described technique of signal detection measures the final color of the image, as the true color of luminescence on the specimen, and the gray level of the image is tuned by the BSE-signal value

which reflects the specimen topography. The dynamic interval of the final signal is limited by the capability of the human eye to perceive and balance between CCL and BSE contrast that is fixed by amplification coefficients in the R-, G-, B-, and Y channels. Using others SEM modes, we can apply the above principle to different signals, for example, the induced current signal (Y-channel) + (CCL mode for RGB-channels), and so forth.

Composite CCL+BSE contrast in scanning microscopy is a new type of SEM mode that is a fairly promising tool for the investigation of luminescence materials. The (CCL + BSE) – SEM images with both fine structure and color information may be able to simplify the observation, interpretation, and analysis of different nature specimens, since the human eye is essentially an organ for observing color and can distinguish thousands of color hues and intensities.

The following literature can be used for further CL reading [6–8].

## 3. Results and discussion

### *3.1. Structure, morphology, and luminescence of $SrAl_2O_4:Eu^{2+}$, $Dy^{3+}$*

Figure 5 shows the main XRD patterns of $SrAl_2O_4:Eu^{2+}$, $Dy^{3+}$ annealed in an active carbon atmosphere at 1250°C for 2 h.

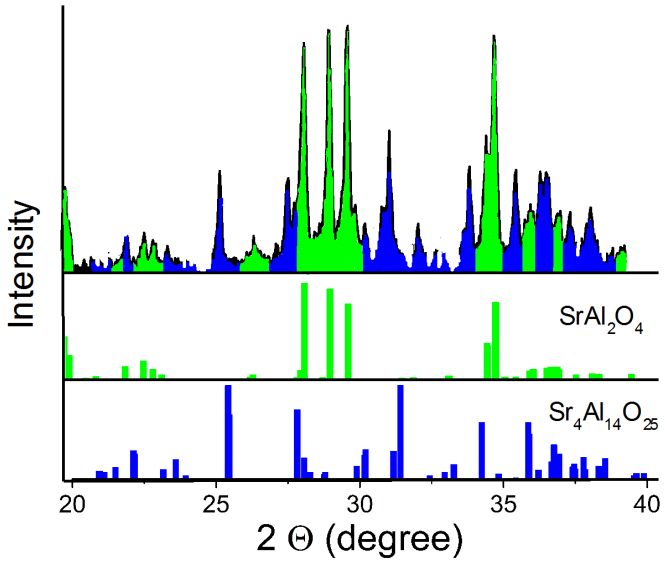


**Fig. 5.** XRD patterns of the synthesized phosphor.

It is evident from Fig. 5 that the XRD patterns include two phases—$SrAl_2O_4$ and $Sr_4Al_{14}O_{25}$—indicating the formation of mixed oxide phases. With an increase in the firing temperature to 1250°C, the XRD peaks becomes sharper and stable phases of $SrAl_2O_4$ and $Sr_4Al_{14}O_{25}$ with higher crystallinity can be obtained.

PL spectroscopy indirectly confirms the presence of two phases. The detailed results of

these experiments are given in our previous papers [9–11]. Here, in Fig. 6, we show the emission spectra of the synthesized phosphor.

The asymmetry of PL emission intensity allows us to decompose this spectrum into blue and green bands peaking around 490 and 520 nm. These bands correspond to $Sr_4Al_{14}O_{25}$ (490 nm) and $SrAl_2O_4$ (520 nm) phases doped with $Eu^{2+}$.

The direct confirmation of this hypothesis follows from CL measurements. The results of experimental investigations of the prepared phosphors by secondary electrons, CCL, and a combined signal are presented in Fig. 7. In all the experiments, the accelerating voltage in SEM was 20 kV and the beam current was 100 nA. The diameter of the electron beam did not exceed 0.1 μm. We used a recording system consisting of three multipliers with different light filters (R, G, B) and a multichannel device connected to photomultipliers. It allows simultaneous transmission of video signals on all channels in any pre-determined range of the spectrum. Images of the surface under study and the respective CL emission from the surface were displayed on video monitors.

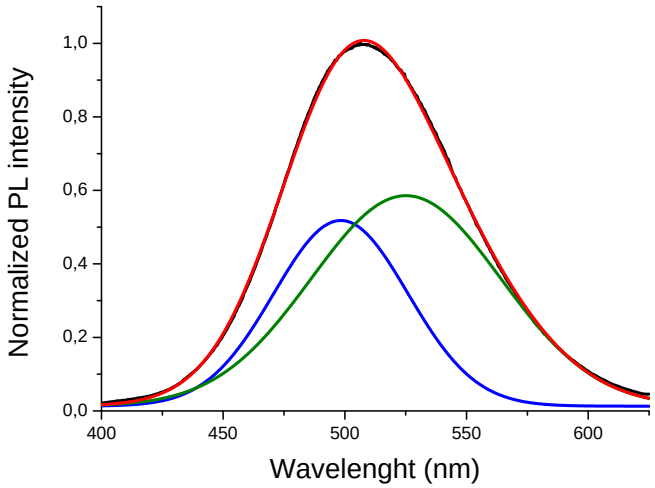


**Fig. 6**. Decomposition of total PL intensity into blue and green bands.

In secondary electrons (Fig. 7a) we can see only the topography of agglomerated powder. CCL (Fig. 7b) shows the spatial distributions of different CL spectral bands (green 520 nm and blue 490 nm) corresponding to $SrAl_2O_4$:$Eu^{2+}$, $Dy^{3+}$ and $Sr_4Al_{14}O_{25}$:$Eu^{2+}$, $Dy^{3+}$, respectively. This direct experiment really confirms the existence of two different phases with different colors. Moreover, the absence of red color centers proves that the entire $Eu^{3+}$ was reduced to $Eu^{2+}$ during synthesis. The combination of CCL with the secondary electron image (Fig. 7c) provides comparison of the analytical CL image with the surface topography of the sample.

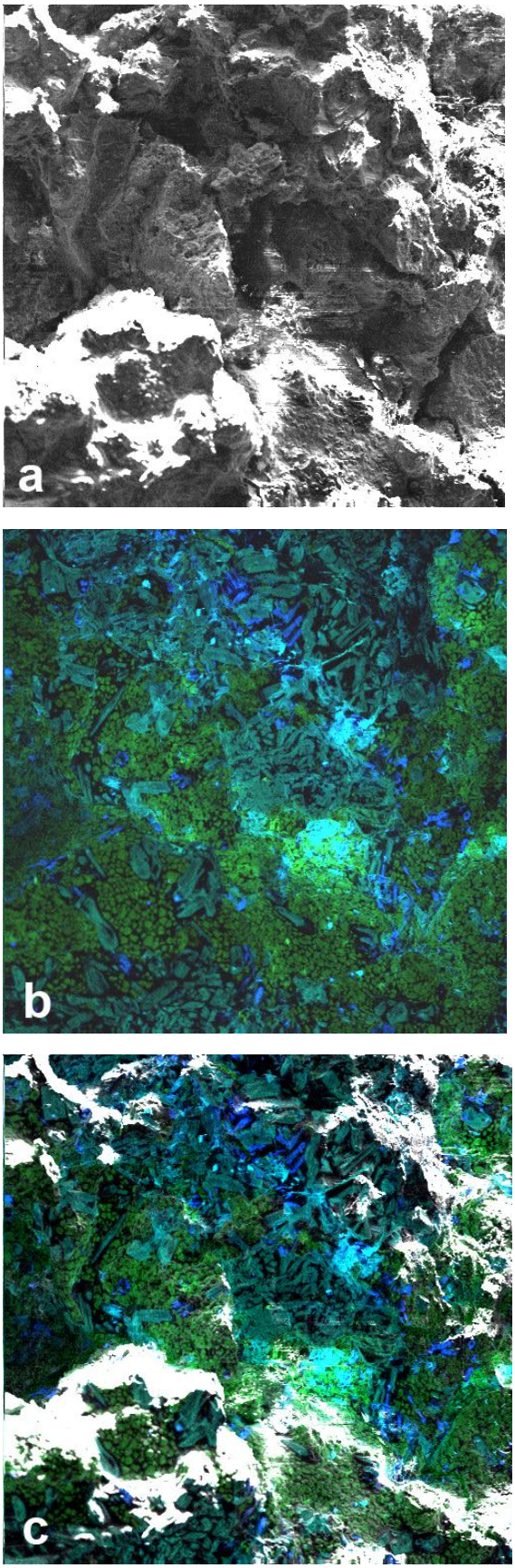


**Fig. 7.** CCL-SEM images of $SrAl_2O_4:Eu^{2+}$, $Dy^{3+}$ in different modes: (a) secondary electrons (SE), (b) CCL, and (c) SE + CCL. Horizontal field width = 1000 μm.

### *3.2. CCL of artificial diamonds*

To demonstrate the advantages of the CCL method in comparison with the black/white contrast, we present some examples of different types of materials that we examined: II–VI and III–V compounds, I–V group semiconductors, ceramics, phosphors, minerals, biomedical specimens, etc. For example, Fig. 8 shows the CCL images of some artificial diamonds.

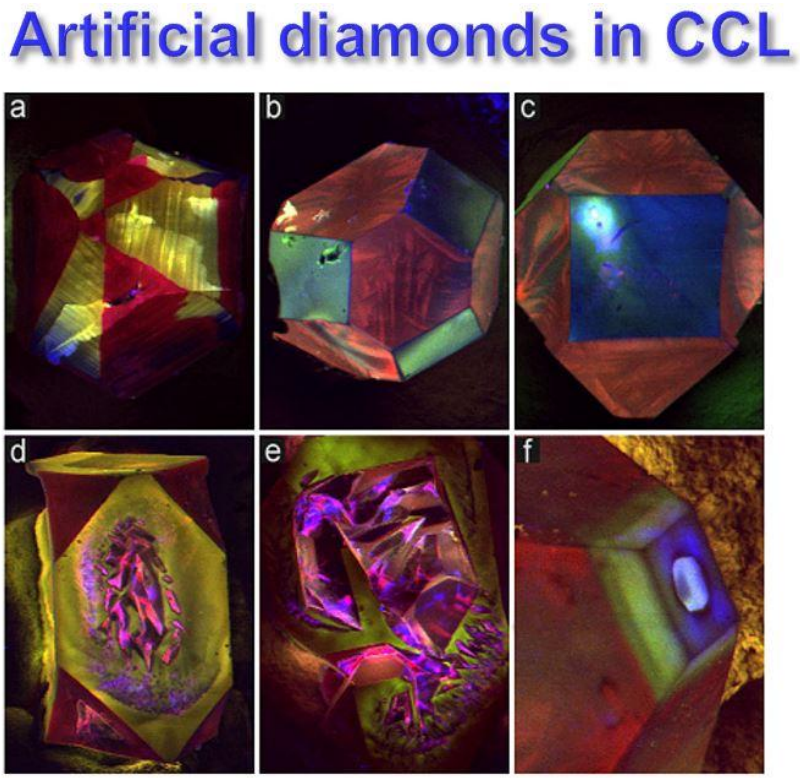


**Fig. 8.** CCL images of some artificial diamonds.

The information capacity of a real CCL image is more than two orders of magnitude higher than that of a black-and-white image used in commercial SEM machines. The detection limit of dopant concentration can be 10 at/cm, which is four orders of magnitude lower than that of the X-ray analyzer and SIMS technique. The sensitivity to the B/C ratio (for diamonds) is 1 ppm; a color contrast image for contrast intervals of $0 < K < 5\%$ is able as black/white contrast image for $K > 5\%$ only; time express analysis: 6 s (frame time); spatial resolution is 0.2 + 0.5 mm for bulk materials and better than the optical resolution for fine materials; the unique CCL-unit design allows interfacing with most SEM instruments. The CCL-system consists of the following components: (1) a SEM specific specimen 12-position stage including an optical mirror, fiber optics, a light detector, and preamplifiers; (2) microprocessor based control and readout electronics; and (3) a video display with a keyboard input.

The main available applications are as follows.

—Microanalysis of materials, mapping of defects, measurement of their densities, impurity segregation studies.

—Acquisition of information on the electronic energy band structure, analysis of luminescence centers and composition.
—Measurement of dopant concentration, minority carrier diffusion length, minority carrier life-time and carrier life-time mapping.
—Analysis of semiconductor devices, analysis of degradation of optoelectronics devices (laser target, light emitting diodes, solid detectors, solar cells, etc.).
—Depth resolved (3D) analysis of defects in ion-implanted samples and epitaxial multilayers.
—Evaluation of various types of diamonds (natural and synthesized diamonds, CVD-diamond films and related materials, such as SiC, etc.) because it distinguishes the type, size and distribution of defects within a crystal on a color monitor.
—Characterization of diamond films; the CCL–SEM technique is available to investigate the B/C ratio, local concentration of dopants, and spatial distribution of the dopant in diamonds. The impurity concentration and structural imperfection should be strictly controlled to obtain the required thermal, optical, or electrical properties, i.e., diamonds with new characteristics.
—Certification (finger print) of gem-quality and tool-quality diamonds.

## 4. Conclusions

A number of advantages of real color contrast application in the SEM in comparison with the black/white contrast for local CL-microanalysis of materials have been shown.

Strong and bright green luminescence has been observed and registered from $SrAl_2O_4:Eu^{2+}$ $Dy^{3+}$ in different modes.

PL and CCL-SEM have been used for the complex examination of $SrAl_2O_4:Eu^{2+}$ $Dy^{3+}$ powder luminescent materials.

CL images obtained in SEM in real colors can be used for a rapid examination of spatial and spectral characteristics of powder and bulk materials produced by different technologies. This method can be recommended as a useful tool in electron microscopy for the complex investigation of luminescent materials.

## References

[1] J. V. Smith and R. C. Stenstrom, J. Geol. 13, 627, (1965).
[2] G. V. Saparin and S. K. Obyden, Eur. Microsc. Anal. **7**(3), 7, (1993).
[3] T. A. Nazarova, G. V. Saparin, S. K. Obyden, and P. I. Ivannikov, Scanning 19(1), 48 (1997).
[4] M. V. Nazarov, T. A. Nazarova, G. V. Saparin, and S. Obyden, Eur. Microsc. Anal. 12(4), 21, (1998).
[5] S. K. Obyden, P. V. Ivannikov, and G. V. Saparin, Scanning 19, 533, (1997).
[6] B. G. Yacobi. and D. B. Holt, Cathodoluminescence Microscopy of Inorganic Solids, Plenum, New York, 1990.
[7] L. Ozawa, Cathodoluminescence: Theory and Applications, VCH, Basel, 1991.
[8] L. Ozawa, Cathodoluminescence and Photoluminescence: Theories and Practical Applications, CRC Press, Boca Raton, 2007.

[9] Nor Nazida, M.N. Ahmad-Fauzi, M. Nazarov, A. Azizan, and K. Shah, Mold. J.Phys. Sci. 11, 1–2, 78, (2012).
[10] S. C. M. Calyn, M. Nazarov, A. Nor Nazida, and M.N. Ahmad-Fauzi, Mold. J. Phys. Sci. 11,1–2, 112, (2012).
[11] M. Nazarov, A. Nor Nazida, A. Azizan, K. Shah Rizal1, S. C. M. Calyn, and M.N. Ahmad-Fauzi, Mold. J. Phys. Sci. 11, 1–2, 67, (2012).